Hydrophobic Polymerized Ionic Liquid for Trace Metal Solid Phase Extraction: Thallium Transfer from Hydrochloric Acid Media

Journal:	*New Journal of Chemistry*
Manuscript ID	NJ-ART-02-2019-000689.R1
Article Type:	Paper
Date Submitted by the Author:	18-Apr-2019
Complete List of Authors:	Tereshatov, Evgeny; Texas A&M University, Cyclotron Institute Boltoeva, Maria; Université de Strasbourg, IPHC, ; CNRS, UMR 7178, Mazan, Valérie; CNRS, Radiochimie Baley, Colton; Texas A&M University, Cyclotron Institute and Department of Nuclear Engineering Folden III, Charles; Texas A&M University, Cyclotron Institute, Department of Chemistry

Hydrophobic Polymerized Ionic Liquid for Trace Metal Solid Phase Extraction: Thallium Transfer from Hydrochloric Acid Media

Evgeny E. Tereshatov,[a,*] Maria Boltoeva,[b] Valérie Mazan,[b,1] Colton Baley,[a,c,2] Charles M. Folden III[a,d]

[a]*Cyclotron Institute, Texas A&M University, College Station, TX 77843 USA*

[b]*Université de Strasbourg, CNRS, IPHC, UMR 7178, F-67000 Strasbourg, France*

[c]*Department of Nuclear Engineering, Texas A&M University, College Station, TX 77843 USA*

[d]*Department of Chemistry, Texas A&M University, College Station, TX 77843 USA*

[*]*E-mail address of the corresponding author: etereshatov@tamu.edu*

[1]*Present address: Université de Strasbourg, CNRS, LIMA, UMR 7042, F-67087 Strasbourg, France*

[2]*Present address: University of Texas Health Science Center at San Antonio, San Antonio, TX 78229 USA*

Abstract

It is known that some neat room-temperature hydrophobic ionic liquids can extract metallic species from aqueous solutions. The unique properties of such organic media allow for the application of polymerization techniques to convert the liquid organic phase to a solid one. In this work, a pyrrolidinium-based ionic liquid and a corresponding polymer with *bis*(trifluoromethanesulfonyl)imide counter anion have been considered for optimization of thallium(III) migration in liquid-liquid and solid-liquid extraction systems. Neither trivalent indium nor monovalent thallium were absorbed by the polymer layer. A mathematical model to describe the mechanism of metal extraction in these systems has been developed. Thermodynamic parameters as adsorption enthalpy, entropy, and Gibbs energy have also been determined.

1 Introduction

There is a demand from an environmental and technological point of view to find safe alternatives for conventional solvents because the commonly used ones are usually toxic (for example, benzene, toluene), volatile (for example, acetone, alcohols) and flammable (for example, kerosene, diethyl ether).[1] As a result, a new class of compounds, so-called ionic liquids (ILs), was developed. Ionic liquids are organic salts, formed by discrete cations and anions, with a melting point below 100 °C.[2] A considerable fraction of such salts are liquid at room temperature, and this provides an opportunity to apply them in a variety of applications[3] (either as a replacement for a traditional organic solvent or a unique additive to a known system), resulting in a drastic change in a given analyte's distribution behavior. In some cases, neat ILs can play an additional role of organic media with a very high affinity for the compound of interest.[4, 5] There is a significant group of ILs that are immiscible with water, and this determines their application in diverse extraction processes. Usually, the hydrophobicity of such ILs is induced by fluorinated anions. The latest generation of these anions [for example, *bis*(trifluoromethanesulfonyl)imide, *bis*(fluorosulfonyl)imide] is stable under experimental conditions

with no tendency to be hydrolyzed and to release hydrofluoric acid. However, carbon-fluorine bonds are practically non-biodegradable, which makes these materials a major pollutant.[6, 7] An alternative route to achieve hydrophobicity is to implement long carbon chain radicals to either carboxylic anions or tetraalkylammonium/tetraalkylphosphonium cations and their combinations.[8, 9] The presence of unsaturated carbon-carbon bonds allows for polymerization reactions to produce solid compounds with characteristic properties. This transformation allows for coating a desired surface with a thin polymer layer suitable for solid-phase extraction. This is important because the liquid-liquid extraction technique usually requires vigorous phase mixing, generates large volumes of waste and sometimes can lead to a third phase formation, while solid-phase extraction consumes smaller volumes of toxic compounds and may result in higher enrichment factors.[10, 11]

Today, diallyl- and vinyl-containing compounds (for example, 1-vinylimidazole) are reasonably considered as monomers for production of pyrrolidinium or imidazolium-based polymers, respectively, due to the relative ease of breaking double carbon-carbon bonds.[12, 13] Length control of the two other alkyl chains attached to the nitrogen atom in the ammonium salt allows one to synthesize diverse pyrrolidinium-based polymers.[14] Photopolymerization and complex high temperature methods are usually used in laboratory production of the desired compounds.[15] However, there are commercially available polymers, for example in acetone solution, which are immediately suitable for coating processes because solvent evaporation leads to a polymer layer covering the surface of interest. Lately, ionic liquids have become very popular stationary phases[16] due to their unique properties for preparation of wall-coated[17] and monolithic columns.[18] Also, to increase the surface area and intensify the separation processes inside the wall-coated tubes, different materials can be added, for example zeolites, active carbon, silica gel[11, 19] and glass beads.[11, 19-22] There are two general methods described in the literature on inner surface coating of either glass or plastic tubes, namely static[23, 24] and dynamic.[25, 26] The former technique requires one end of the tube to be closed while the tube is filled with a mixture containing a volatile solvent and the desired coating material, and then the tube is placed under vacuum to slowly evaporate the solvent. The latter method is based on the slow motion of a liquid plug that consists of the same mixture of solvent and coating material to wet the inner surface of the tube.

Indium and thallium have growing economic needs from high-tech industries for the manufacture of liquid crystal displays[27, 28] and environmental protection.[29, 30] Also, both elements have medical radioisotopes (In-111 and Tl-201) available for *in vivo* diagnostic imaging and radioimmunotherapy procedures and cardiological imaging exams, respectively.[31, 32] Macro amounts of indium salts are highly toxic when administered subcutaneously or intravenously.[33] Thallium is also known to be highly toxic and biogeochemically mobile metal.[34] Thus, the content of indium and thallium in environmental systems has to be strongly regulated and controlled. Permissible exposure limits for indium and its compounds according to the U.S. Occupational Safety and Health Administration[33] are 0.1 mg/m^3 and the maximum thallium contamination level in drinking water is 2 μg/L.[35]

Despite that polymerized ionic liquids are widely used in diverse technological fields (environment, energy, catalysis, etc.),[36, 37] particularly in analytical chemistry, to the best of our knowledge there are only a few articles on their utilization for solid-phase extraction of metals.[38, 39] The goal of this work is to

expand the field and perform a proof-of-principle experiment that polymerized ionic liquids are effective and selective separation media for metals, and to study mechanisms of analyte adsorption.

2 Experimental

2.1 Chemical reagents

All chemicals were reagent grade and used without additional purification unless noted otherwise. Aqueous solutions were prepared using deionized water (from an ELGA PURELAB DV25) with a resistivity of 18.2 MΩ cm. The ionic liquid *N*-propyl-*N*-methylpyrrolidinium *bis*(trifluoromethanesulfonyl)imide (abbreviated hereafter as $[C_3C_1pyrr][Tf_2N]$, 99.5% purity), the powder poly(diallyldimethylammonium) *bis*(trifluoromethanesulfonyl)imide ($[PDDA][Tf_2N]_n$, 99.9% purity), the liquid mixture of poly(diallyldimethylammonium) *bis*(trifluoromethanesulfonyl)imide and *N*-butyl-*N*-methylpyrrolidinium *bis*(trifluoromethanesulfonyl)imide in acetone (60:40 wt ratio, $[PDDA+C_4C_1pyrr][Tf_2N]_n$, 99.9% purity), and the salt lithium *bis*(trifluoromethanesulfonyl)imide ($LiTf_2N$, >99% purity) were purchased from Solvionic (Toulouse, France). The chemical structures of the ionic liquids and ions investigated in the present work, along with the shorthand notation used to represent them, are depicted in Fig. 1.

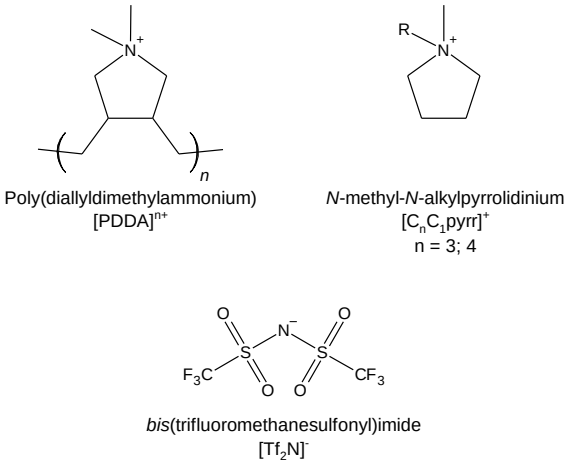

Fig. 1 Structures, names and abbreviations of ionic liquids' cations and anions employed in this study.

Ultra-pure acetone was purchased from Fisher Scientific and Tl(III) chloride hydrate salt from Alfa Aesar. Hydrochloric acid (35 wt%) was supra quality grade (Roth). Biotechnology grade AG® 50W-X8 resin (biotechnology grade, 200-400 mesh, hydrogen form) was purchased from BIO-RAD. Its density and ion exchange capacity are 0.80 g/mL and 1.7 meq/mL, respectively. Deuterium oxide (D_2O, Eurisotop), deuterium chloride (deutero-hydrochloric acid, DCl, 35 wt% in D_2O) of analytical grade (purchased from Sigma Aldrich) were of 99 atom% purity of deuterium. Sodium trifluoroacetate (98%) was purchased from Alfa Aesar.

2.2 Surface coating with a polymer

The inner surface of a PTFE tube (∅ 4 mm) was coated using the $[PDDA+C_4C_1pyrr][Tf_2N]_n$ mixture in acetone. Tubes of the desired length (~25 cm) were washed with water and dilute nitric acid (0.2 M) to prepare the surface for coating. Then, one end of a tube was plugged and ~0.5 g of

[PDDA+C_4C_1pyrr][Tf_2N]$_n$ mixture in acetone were transferred to the tube along with an additional amount of acetone to fill ~20 cm of the tube. After that, the tube was placed into a rotary evaporator while the acetone was slowly (~2 h) evaporated under moderate vacuum at 280 rpm. The same technique was implemented when glass beads (≤ 106 μm, 425 – 600 μm and 1 mm diameter) were added into the tube.

2.3 Polymer film characterization

After the surface coating was finished, a PTFE tube was cut in two semicylinders to have access to the film prepared. A small piece of the polymer was taken for the SEM analysis, where the film was metal coated (80% Pt/20% Pd) in a 208HR High Resolution Sputter Coater prior to analysis to eliminate charging and to improve contrast on the low-density material.

2.4 Radioisotopes

Some experiments utilized radionuclides for analysis. Carrier-free thallium-201 (half-life 3.04 d, 70.8 keV X-ray, 46% intensity) and indium-111 (half-life 2.80 d, 245.5 keV gamma-ray, 94% intensity) medical radioisotopes were purchased from Mallinckrodt (St. Louis, Missouri, USA). The production methods are ^{203}Tl(p,3n)^{201}Pb → ^{201}Tl and ^{112}Cd(p,2n)^{111}In, respectively. Thallium chloride is in 0.9 % (w/v) sodium chloride and preserved with 0.9 % (v/v) benzyl alcohol and indium chloride is in 0.05 M hydrochloric acid. The activity was detected using a PerkinElmer NaI automated gamma-counter.

2.5 Thallium oxidation state

The thallium oxidation state in the Tl-201 stock solution was assigned to +1 according to our previous work.[40] Chlorine water was used in order to maintain the highest thallium oxidation state (+3) during the experiments with radioactive thallium.

An aqueous stock solution of stable Tl(III) was prepared by dissolving a given quantity of $TlCl_3 \cdot H_2O$ salt in 0.2 M HCl. An analytical balance (Sartorius, BP 2215 model) with an accuracy of ± 0.1 mg was used for weighing the components. This solution was placed in contact with 4 g of AG® 50W-X8 resin overnight under agitation. Beforehand, the resin was conditioned three times with 0.2 M HCl during 2 hours to absorb monovalent thallium according to a procedure described elsewhere.[41] Immediately after cation exchange, the prepared solution of Tl(III) was filtered using a 0.2 μm filter. If it was needed or desired, the aqueous acid concentration was adjusted by adding concentrated HCl. The metal extraction experiments were carried out with minimal delay in order to avoid Tl(I) formation in the solution.

2.6 Preparation of a flat polymer film for the batch studies

Approximately 0.15 g of [PDDA][Tf_2N]$_n$ powder was completely dissolved in acetone and then this solution was transferred to a polytetrafluoroethylene (PTFE) beaker. The solution was subjected to slight heating and, after the evaporation of the solvent, a white film was formed at the bottom of the beaker. This hydrophobic polymeric IL film was peeled off and then dried under vacuum at 0.5 mbar until constant weight. This film was used in extraction study with stable Tl(III).

Also, approximately 0.5 g of the [PDDA+C_4C_1pyrr][Tf_2N]$_n$ mixture in acetone were transferred into a glass beaker where the solvent was evaporated to dryness in a fume hood. This film was used later for separate batch extraction tests with the radioactive indium and thallium radioisotopes.

2.7 Analytical procedure

The hydrophobic ionic liquid [C_3C_1pyrr][Tf_2N] was dried prior to use under vacuum following a previously published procedure.[42] The content of residual water was less than 0.03 wt%. The hydrochloric acid solutions were prepared by diluting concentrated HCl with deionized water to the desired concentration.

The metal distribution ratio measurements were performed by a standard liquid-liquid extraction technique. Generally, equal volumes of IL and aqueous phase (generally 0.8 mL) were placed into Eppendorf centrifugation tubes (2 mL). The corresponding IL masses were calculated using the known density of [C_3C_1pyrr][Tf_2N] ionic liquid (1.40 g/mL according to the manufacturer) and were taken precisely by weighing. The aqueous acidic solution of Tl(III) was added into the tube using an Eppendorf Research precision pipette. The biphasic samples were vigorously mixed for 1 hour at 1,500 rpm on a mechanical shaker (IKA vibrax VXR basic). After a given shaking time, the samples were centrifuged for 4 min at 7,500 rpm (Micro Star 12, VWR) in order to promote phase separation. Then, aliquots of each phase were taken for further analysis.

The solutions of LiTf_2N were obtained by exact weighing of a calculated amount of powder and dissolving in a volumetric flask in 1 M HCl.

The deutero-hydrochloric solutions were prepared by diluting concentrated DCl with deuterium oxide to the desired concentration.

The aqueous concentrations of protons were determined by acid-base titration (SCHOTT instrument Titroline easy) using NaOH standard solutions (Carlo Erba).

The stable Tl(III) concentrations in the stock and working aqueous solutions were determined by inductively coupled plasma mass-spectroscopy (ICP-MS, Varian 7500 series) after dilution to a concentration suitable for measurements in 0.01 M HCl solution. This solution also contained 10 µg/L holmium (Ho) as an internal standard.

The aqueous [Tf_2N^-] anion concentration was determined by fluorine-19 (^{19}F) quantitative nuclear magnetic resonance (qNMR) measurements with 5% relative uncertainty.[43] The NMR spectra were collected with a Bruker AVANCE I 300 MHz spectrometer with a 5 mm PABBO BB-1H/D Z-GRD probe at 25°C under analytical conditions.

2.8 Distribution ratio measurements

All measurements in this study were performed at room temperature (23 ± 2°C) unless stated otherwise.

The distribution ratio of metal ions between two immiscible phases was calculated according to the following equation:

$$D_M = \frac{[M]_{init} - [M]_{eq}}{[M]_{eq}} \quad \text{Eq. 1}$$

where $[M]_{init}$ and $[M]_{eq}$ are initial and equilibrium metal ion concentrations (mol/L) in the aqueous phase, respectively.

When a radioactive tracer was used, the extraction efficiency was determined as

$$E_M = \frac{A_{init} - A_{eq}}{A_{init}} \cdot 100\% \quad \text{Eq. 2}$$

where A_{init} and A_{eq} are initial and equilibrium aqueous phase activities (Bq).

2.9 Static solid-liquid extraction

For some solid-liquid extraction experiments, 1 mL 0.05 M HCl containing either Tl-201 or In-111 was transferred to a beaker with a dry [PDDA+C_4C_1pyrr][Tf_2N]$_n$ polymer at the bottom. This solution completely covered the polymer film. Manual shaking was applied for 3 min to intensify metal diffusion toward the film. The activity of the radioactive solutions was measured before and immediately after contact with the polymer. The calculated activity ratio indicated the efficiency of metal extraction. The same beaker and the same polymer were used in these tests.

2.10 Dynamic solid-liquid extraction

For the solid-phase extraction experiments, a small piece of [PDDA][Tf_2N]$_n$ film (approximately 50 mg) was first cut off and precisely weighed in 2 mL test tube. One milliliter of Tl(III) aqueous acidic solution was then added to the tube. Samples were mixed for 1 h at 100 rpm on a mechanical shaker (IKA vibrax VXR basic), and then the aqueous acidic phase was withdrawn for further analysis. In the temperature-dependent experiments, another shaker was used [Thermo-Shaker TS-100 (Biosan)].

3 Results and Discussion

3.1 Tube inner surface coating

It was found that the static method to coat inner surfaces is more effective[26] and this technique was chosen in our work. One expected disadvantage of the static method is time required for the coating. It was previously reported[24] that it takes up to 3 d to evaporate the solvent from a ∅ 0.2 mm x 20 m glass capillary. In our experiments, the PTFE tube used is ∅ 4 mm x 20 cm and the preparation of a thin [PDDA+C_4C_1pyrr][Tf_2N]$_n$ film takes approximately 2 h.

The analysis of the polymer found on the inner surface of the PTFE tube (Fig. 2a) revealed that the film thickness is approximately 6 mg/cm^2. The material deposited was distributed along the tube due to its constant rotation at 280 rpm while being under vacuum. However, the thickness of the layer (Fig. 2b) can be controlled by varying the amount of the polymer in the tube prior to the solvent evaporation.

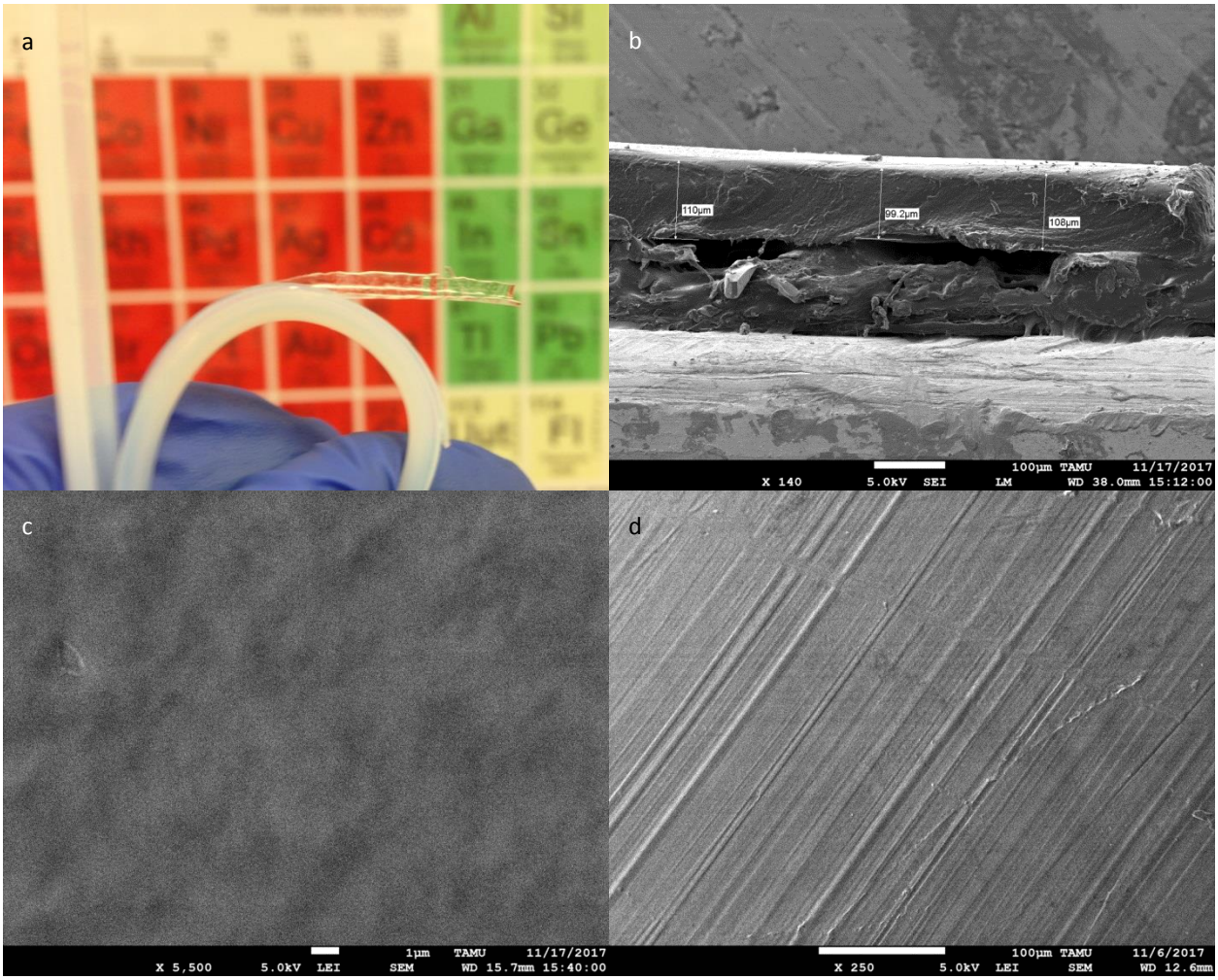

Fig. 2 SEM images of the film obtained: a – a photograph of a PTFE tube (cut in two semicylinders) with a polymer film inside, b – SEM-based analysis of the layer thickness; a piece of the polymer was placed on top of the adhesive material to prevent curvature and the assembly was positioned vertically for ease of measurement, c – SEM image of the inner surface of the polymerized film, d - SEM image of the outer surface (facing the tube wall) of the polymerized film.

Scanning electron microscopy was also used to study the surfaces of the films obtained. It is important to distinguish between the surface in contact with the tube wall and the surface exposed to the medium inside the tube. The latter surface is shown in Fig. 2c. There is no obvious porosity found even at 5500 magnification. The surface seems to be smooth; no cracks or cavities were detected. This fact is important in terms of minimal physisorption of the analyte of interest (discussed below). The opposite surface (facing the PTFE tube) has an imprint of the plastic tube, noticeable even at much lower magnification (Fig. 2d). This tube roughness likely aids the polymer film adhesion due to the increase in surface area. Thus, the open tube with the polymer inside was fabricated and the surfaces obtained were characterized.

3.2 Pseudomonolithic column with polymer

According to the procedure described above, a pre-polymerized pyrrolidinium-based [PDDA+C_4C_1pyrr][Tf_2N]$_n$ ionic liquid was used to coat the inner tube surface. In order to create increased surface area and to add porosity to the inner body of the column, glass beads were added to the tube

with the polymer and the solvent mixture as discussed above. The procedure calls for soaking the beads in the acetone–poly(IL) mixture at least overnight prior to the forced solvent evaporation; this will wet the inner wall of the tube and the outer surface of the beads while preventing air plug formation. Since the mass of the polymer used was almost the same regardless of whether beads were present or absent, in the former case the polymer film thickness must be less due to the added surface area. Moreover, the continuous spinning of the tube and corresponding centrifugal force result in uneven film profile from the tube axis towards the wall. Figure 3a shows the 425 – 600 μm beads before they were polymer coated. Figure 3b shows the thickness of the polymer film peeled off one of the beads after coating. Based on the SEM measurements, the film thickness was estimated to be approximately 4 μm. Fig. 3c shows how the polymer-coated beads are oriented and connected to each other by the polymerized ionic liquid. Each bead has at least one neck-shaped bond that holds all of the beads together, prevents them from moving and determines the pore structure. These pores are open because a simple test reveals that water can easily pass through such a column. Also, Fig. 3d indicates how the beads are connected to the column wall; similar neck-shaped structures allow the entire assembly to attach to the inner surface of the tube. However, the parietal polymer layer thickness was found to be ~30 μm (not shown in the figure). This is almost 1/3 of the layer thickness without any beads in the tube. Since the initial poly(IL) concentration is the same in both cases, the other 2/3 of the mass is utilized in the beads' coating.

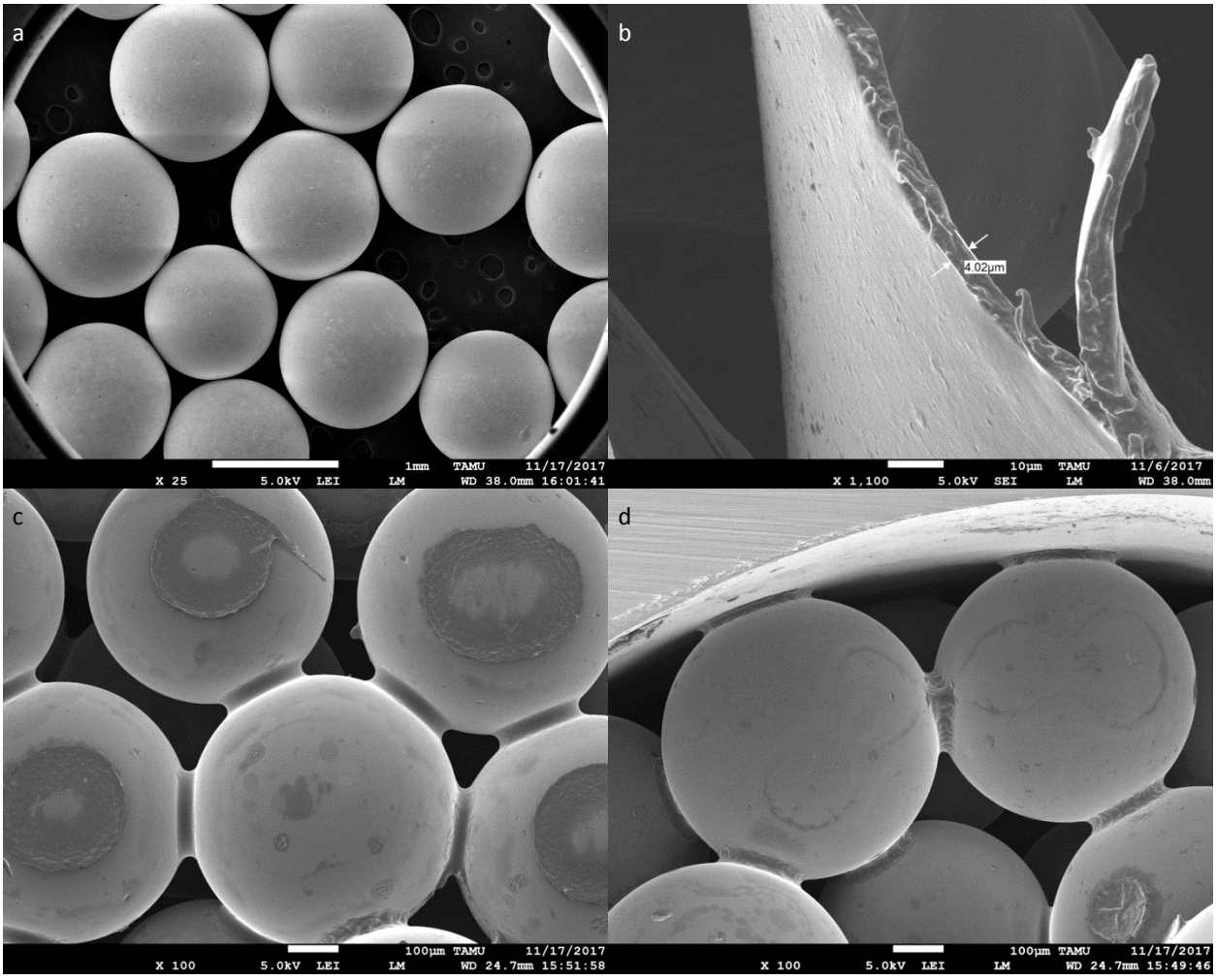

Fig. 3 SEM images: a – glass beads (1 mm diameter) before the polymer coating, b – thickness of the polymer layer on the beads; after solvent evaporation, the tube was cut and the coated beads were analyzed. In some cases the polymer was partially peeled off the beads, c – micrograph of the polymer-coated beads showing neck-shaped bonds between the multiple beads, creating an open pore system, d – micrograph of the neck-shaped bonds between the beads and the PTFE tube wall, which helps to retain the beads in the column.

3.3 Aqueous solubility of polymerized and non-polymerized ionic liquid

The aqueous solubility of the hydrophobic pyrrolidinium-based poly(ionic liquid), $[PDDA][Tf_2N]_n$, is one of the most important factors, because the presence of the IL ions in the aqueous phase determines the extraction of the desired species.[43, 44] This particular ionic liquid was chosen to study the solubility of 100% polymerized IL without incorporation of the $C_4C_1pyrr^+$ hydrophilic cation, because the absence of non-polymerized ionic liquid in the polymer should help to better understand the solubility process and as a result the mechanism of metal extraction driven by the polymerized ionic liquid only. The influence of the aqueous phase acidity on the solubility of the $[PDDA][Tf_2N]_n$ film was investigated in the 1 – 7 M HCl range. Unfortunately, evaluation of the concentration of the cationic IL moiety using quantitative ^{1}H-NMR was complicated because of a very low signal intensity, and only the aqueous concentrations of fluorine-containing species (Tf_2N^- and HTf_2N) at equilibrium were measured.

It is known that protonation of Tf_2N^- anions occurs in acidic media according to

$$H^+_{aq} + Tf_2N^-_{aq} \rightleftarrows HTf_2N_{aq} \quad \text{Eq. 3}$$

The HTf_2N acid dissociation constant, K_a, was found to be 0.70 ± 0.04 mol dm^{-3}.[45] To evaluate the concentrations of individual species, a system of equations (Eq. 4) was developed. This system is similar to one proposed in our previous publication[46] and is based on mass balance and the dissociation constant of HTf_2N from Eq. 3. The mean ionic activity of HCl ($\gamma_{HCl\pm}$) was used as the activity coefficient of the protons and the data were taken from literature.[47] Proton- and fluorine-containing species are referred to as $H_{Titrated}$ and F_{NMR}, respectively.

$$\begin{cases} [H^+]_{aq} + [HTf_2N]_{aq} = [H_{Titrated}] \\ [Tf_2N^-]_{aq} + [HTf_2N]_{aq} = [F_{NMR}] \\ \dfrac{\gamma_{HCl\pm} \cdot [H^+]_{aq} \cdot [Tf_2N^-]_{aq}}{[HTf_2N]_{aq}} = K_{a_{[HTf_2N]}} \\ \gamma_{HCl\pm} = f\left([H^+]_{aq}\right) \end{cases} \quad \text{Eq. 4}$$

Figure 4a shows the measured behavior (based on Eq. 4) of the corresponding individual species for both IL and poly(IL) dissolution in HCl media. It is evident that Tf_2N^- protonation takes place (Eq. 3), resulting in HTf_2N formation, and this species dominates in > 1 M HCl solution. For example, at least 90% of the experimentally measured NMR data are attributed to HTf_2N acid in > 3 M HCl region. Figure 4b depicts the cations' solubility of corresponding IL and poly(IL) in HCl media. It is evident that the IL cation concentration increases with increasing aqueous phase acidity and the opposite trend was found for the Tf_2N^- anions. This study demonstrates that there is no perceptible solubilization of the poly(IL) $[PDDA][Tf_2N]_n$ up to 1 M HCl. Above this value and up to 5 M HCl, only upper limits of cation concentration were estimated. Thus, the degradability of the poly(IL) and IL is enhanced with increasing acid concentration.

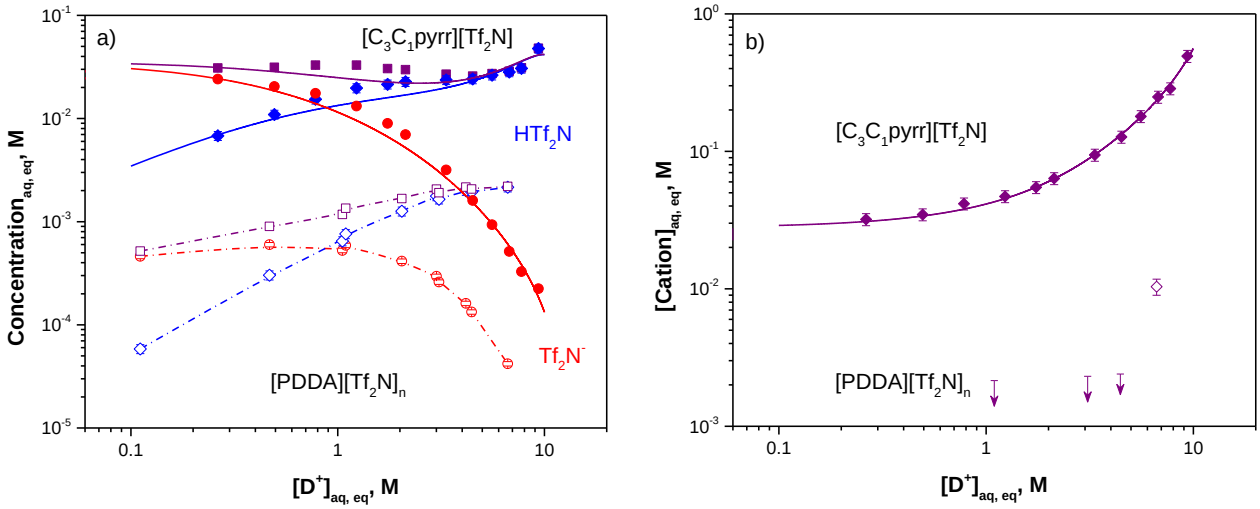

Fig. 4 Effect of aqueous DCl concentration on the solubility of the pyrrolidinium-based ionic liquid $[C_3C_1pyrr][Tf_2N]$ (closed symbols) and the poly(ionic liquid) $[PDDA][Tf_2N]_n$ (open symbols): a – results of ^{19}F-NMR measurements (purple squares) and

calculations according to Eq. 4 of individual equilibrium concentrations of Tf_2N^- (red circles) and HTf_2N (blue diamonds) species; in many cases, the uncertainties are smaller than the corresponding symbols; b – results of ^{1}H-NMR measurements of equilibrium concentrations of the IL and poly(IL) cations. In the case of solid-phase extraction, the solid-to-liquid ratio was 0.025 g/mL. The NMR data for the non-polymerized IL in 1 – 7 M DCl range are taken from our previous article.[43] The solid lines for Tf_2N^- and $C_3C_1pyrr^+$ ions are the results of fitting according to Eqs. 11 and 12, respectively. The solid blue and purple lines in Fig. 4a are combinations of Eqs. 4 and 11. The dash dotted lines are drawn to guide the eye.

Upon dissolution of the IL in up to 5 M HCl, it was confirmed that no detectable Cl^- anion was found in the organic phase.[45, 48, 49] However, in more concentrated HCl solutions, there is evidence of the presence of chloride in the organic phase[46] and we believe this is due to partial extraction of HCl according to the following equation:

$$\mathrm{HCl_{aq}} \rightleftarrows \mathrm{HCl_{org}}, \qquad \text{Eq. 5}$$

where $[HCl]_{org} = K_{ex\_HCl} \cdot [HCl]_{aq} = K_{ex\_HCl} \cdot [Cl^-]_{aq}$. Thus, one more chemical reaction should be considered in the organic phase:

$$[\mathrm{C_3C_1pyrr}][\mathrm{Tf_2N}]_{org} + \mathrm{HCl_{org}} \rightleftarrows [\mathrm{C_3C_1pyrr}]\mathrm{Cl_{org}} + \mathrm{HTf_2N_{org}} \qquad \text{Eq. 6}$$

This reaction leads to formation of a hydrophilic $[C_3C_1pyrr]Cl$ ionic liquid that will be partially back-extracted into the aqueous phase according to:

$$[\mathrm{C_3C_1pyrr}]\mathrm{Cl_{org}} \rightleftarrows [\mathrm{C_3C_1pyrr^+}]_{aq} + \mathrm{Cl^-}_{aq}, \qquad \text{Eq. 7}$$

where $[\mathrm{C_3C_1pyrrCl}]_{org} = [\mathrm{C_3C_1pyrr^+}]_{aq} \cdot [\mathrm{Cl^-}]_{aq}/\mathrm{K_{b\_ex\_C_3C_1pyrrCl}}$.

Thus, the concentration difference between cations and anions of the IL at any given HCl concentration is due to HTf_2N formation, HCl extraction and $[C_3C_1pyrr]Cl$ back-extraction:

$$n \cdot [\mathrm{C_3C_1pyrr^{n+}}]_{aq} - [\mathrm{Tf_2N^-}]_{aq} = [\mathrm{HTf_2N}]_{aq} + \mathrm{K_{ex\_HCl}} \cdot [\mathrm{Cl^-}]_{aq} + [\mathrm{C_3C_1pyrr^{n+}}]_{aq} \cdot [\mathrm{Cl^-}]_{aq}^n/\mathrm{K_{b\_ex\_C_3C_1pyrrCl_n}}, \qquad \text{Eq. 8}$$

where *n* is degree of polymerization (n = 1 for non-polymerized IL). The solubility product is therefore:

$$\mathrm{K_{sp}} = [\mathrm{C_3C_1pyrr^{n+}}]_{aq} \cdot \left([\mathrm{Tf_2N^-}]_{aq} + [\mathrm{HTf_2N}]_{aq}\right)^n = [\mathrm{C_3C_1pyrr^{n+}}]_{aq} \cdot [\mathrm{Tf_2N^-}]_{aq}^n \cdot \left(1 + [\mathrm{H^+}]_{aq}/\mathrm{K_a}\right)^n, \qquad \text{Eq. 9}$$

and one can write:

$$\left(1 + [\mathrm{H^+}]_{aq}/\mathrm{K_a}\right) \cdot [\mathrm{Tf_2N^-}]_{aq}^{n+1} + \mathrm{K_{ex\_HCl}} \cdot [\mathrm{Cl^-}]_{aq} \cdot [\mathrm{Tf_2N^-}]_{aq}^n - \mathrm{K_{sp}} \cdot \frac{n - [\mathrm{Cl^-}]_{aq}^n/\mathrm{K_{b\_ex\_C_3C_1pyrrCl_n}}}{\left(1+[\mathrm{H^+}]_{aq}/\mathrm{K_a}\right)^n} = 0 \qquad \text{Eq. 10}$$

It can be seen that, in the absence of hydrochloric acid in the aqueous phase $\left([\mathrm{H^+}]_{aq} = [\mathrm{Cl^-}]_{aq} = 0\right)$, $\mathrm{K_{sp}} = [\mathrm{Tf_2N^-}]_{aq}^{n+1}/n$. As the anion concentration in the case of poly(IL) dissolution in water is ~$5 \cdot 10^{-4}$ M, the corresponding solubility product constant can be estimated to be $K_{sp\_poly(IL)} < 2.6 \cdot 10^{-7}$ (since the actual degree of polymerization *n* is unknown, *n* > 1) and experimentally measured solubility product constant of non-polymerized ionic liquid (n = 1) $\mathrm{K_{sp\_IL}} = [\mathrm{Tf_2N^-}]_{aq,IL}^2 = (7.0 \pm 0.7) \cdot 10^{-4}$. Thus, the poly(IL) $[PDDA][Tf_2N]_n$ is much less water soluble than the $[C_3C_1pyrr][Tf_2N]$ ionic liquid.

In the case of n = 1 (no polymerization), Eq. 10 is transformed to a quadratic expression with the following solution:

$$[Tf_2N^-]_{aq} = \frac{-K_{ex\_HCl}\cdot[Cl^-]_{aq} + \sqrt{(K_{ex\_HCl}\cdot[Cl^-]_{aq})^2 + 4\cdot K_{sp}\cdot(1-[Cl^-]_{aq}/K_{b\_ex\_C_3C_1pyrrCl})}}{2\cdot(1+[H^+]_{aq}/K_a)} \quad \text{Eq. 11}$$

Similarly,

$$[C_3C_1pyrr^+]_{aq} = \frac{K_{ex\_HCl}\cdot[Cl^-]_{aq} + \sqrt{(K_{ex\_HCl}\cdot[Cl^-]_{aq})^2 + 4\cdot K_{sp}\cdot(1-[Cl^-]_{aq}/K_{b\_ex\_C_3C_1pyrrCl})}}{2\cdot(1-[Cl^-]_{aq}/K_{b\_ex\_C_3C_1pyrrCl})} \quad \text{Eq. 12}$$

The sign before the radical must be positive in order to eliminate non-physical values. It can be seen that Eqs. 11 and 12 are functions with 3 unknown constants; these can be found by fitting the experimental data in Fig. 5 and using the empirically determined relationship $[Cl^-]_{aq} = 1.118 \cdot [H^+]_{aq}^{0.982}$. The results of the fitting are given in Table 1.

Table 1 Calculated solubility product and extraction constants for $[C_3C_1pyrr][Tf_2N]$

Constant	$[Tf_2N^-]$	$[C_3C_1pyrr^+]$
K_{sp}	$(1.27 \pm 0.28)\cdot10^{-3}$	$(7.7 \pm 0.5)\cdot10^{-4}$
K_{ex_HCl}	$(1.2 \pm 0.5)\cdot10^{-2}$	$(1.79 \pm 0.09)\cdot10^{-2}$
$K_{b\_ex\_C_3C_1pyrrCl}$	13.6 ± 2.2	16.4 ± 0.9

As can be seen, the experimentally measured value, $(7.0 \pm 0.7) \cdot 10^{-4}$, and mathematically estimated solubility product constants for $[C_3C_1pyrr][Tf_2N]$ ionic liquid (Table 1) are in good agreement.

3.4 Proof-of-principle of metal extraction by the poly(IL)

According to the procedure described above, solutions containing radioactive isotopes of In, Tl(I) and Tl(III) were placed one-by-one into a beaker with the polymer to study the extraction selectivity of the layer. It was found that the pyrrolydinium-based pure IL does not extract indium and monovalent thallium.[44] Similarly, In and Tl(I) uptake by the film from the same hydrochloric acid solution was found to be negligible. Therefore, the chemical interaction of species in solution and the polymer is extremely weak and lies below the sensitivity of our measurements. Moreover, the absence of In and Tl(I) adsorption also indicates that there is no physisorption of metals on the surface of the polymer. This type of sorption could have been expected in the presence of any pores or cavities, but the SEM pictures showed that the film is a smooth and uniform layer. Nevertheless, Tl(III) is extracted by the polymer in the beaker at a level of 31 $\pm$ 3 %. This trend is in agreement with previous results on Tl(III) extraction into pure pyrrolidinium-based IL.[44] Also, analogous results were observed when a Tl(III) solution was loaded onto the pseudomonolithic column described above; 50% of the radioactive nuclide was retained by the column. However, the suppressed solubility of polymerized cation (see section 3.3) leads to a smaller amount of Tl(III) being extracted compared to the more mobile cation in liquid-liquid extraction. A detailed mechanism of the Tl(III) interaction with a polymerized ionic liquid will be considered below.

3.5 Mechanism of thallium extraction into IL and poly(IL)

3.5.1 Effect of $LiTf_2N$ on metal extraction

Basic principles and theoretical aspects of metal species extraction into IL phases were considered in detail elsewhere.[50-52] One method to obtain more insight into the extraction mechanism is the introduction of a salt into the aqueous phase which has a common cation or anion with the ionic liquid under investigation, for example $LiTf_2N$ for $[Tf_2N^-]$-based ILs or C_{10}mimCl for imidazolium-based ILs.[53, 54] The choice of corresponding compound depends on whether the anionic or cationic species of interest are expected to be predominant under the given chemical conditions. According to the literature,[55] trivalent thallium is predominantly in the form of $TlCl_4^-$and this species is extracted by ionic liquids. However, it must be noted that formation of $TlCl_5^{2-}$ species at elevated HCl concentrations is also possible and the average value of the corresponding stability constant (K_5) found in literature[56, 57] for the reaction below is 0.68:

$$TlCl_4^- + Cl^- \rightleftarrows TlCl_5^{2-} \qquad \text{Eq. 13}$$

There are two possible mechanisms for ionic liquid-based extraction of negatively charged complexes, for example $TlCl_4^-$. One is anion exchange between an anionic species of interest in the aqueous phase and an anion of the ionic liquid:

$$[Tf_2N^-]_{org} + [TlCl_4^-]_{aq} \rightleftarrows [Tf_2N^-]_{aq} + [TlCl_4^-]_{org} \qquad \text{Eq. 14}$$

Another is the ion pair formation. The general equations to estimate extraction constants and proposed mechanisms of ion pairing can be found in previous reports [45, 58-60]. This process occurs between species of interest and counterions of the ionic liquid dissolved in the aqueous phase, followed by transfer into the IL phase. It can be described for anionic solutes as

$$[C_3C_1pyrr^{n+}]_{aq} + n\cdot[TlCl_4^-]_{aq} \rightleftarrows [C_3C_1pyrr^{n+}]_{org} + n\cdot[TlCl_4^-]_{org} \qquad \text{Eq. 15}$$

The distribution ratio for the ion exchange (K_{IE}, Eq. 14) and ion pair (K_{IP}, Eq. 15) extraction mechanisms are defined as

$$D_{Tl(III)} = \frac{[TlCl_4^-]_{org}}{\sum_{i=0}^{5} TlCl_i^{3-i}} = \frac{K_{IE}\cdot[TlCl_4^-]_{aq}}{[Tf_2N^-]_{aq}\cdot\sum_{i=0}^{5} TlCl_i^{3-i}}. \qquad \text{Eq. 16}$$

$$D_{Tl(III)}^{n} = \frac{K_{IP}\cdot[TlCl_4^-]_{aq}^{n}\cdot[C_3C_1pyrr^{n+}]_{aq}}{\left(\sum_{i=0}^{5} TlCl_i^{3-i}\right)^{n}}. \qquad \text{Eq. 17}$$

$$K_{sp} = \left(1 + [H^+]_{aq}/K_a\right)^n \cdot K_{IE}^n/K_{IP}. \qquad \text{Eq. 18}$$

Thus, the function $D_{Tl(III)} = f([Tf_2N^-]_{aq})$ describes the experimental data on the extraction of solutes from the aqueous phase into the ionic liquid phase in the presence of $LiTf_2N$. At a given acid concentration where only negatively charged thallium species exist (for example 1 M HCl), this function can be written

$$\log D_{Tl(III)} = \log [K_{IE}/(1 + K_5 \cdot [Cl^-]_{aq})] - \log [Tf_2N^-]_{aq}. \qquad \text{Eq. 19}$$

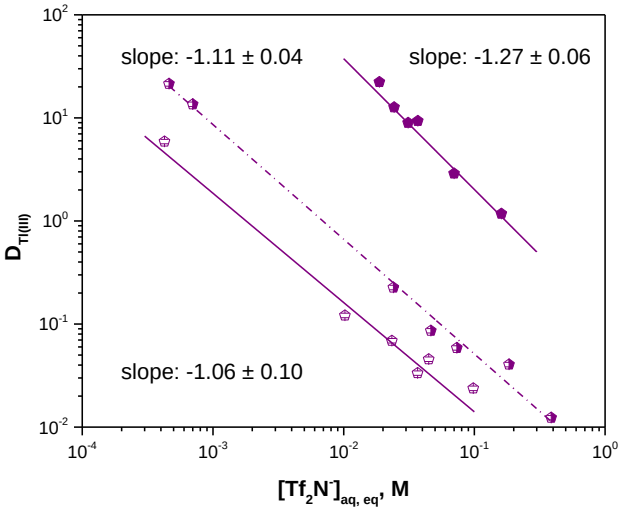

Fig. 6 Effect of $LiTf_2N$ added to the aqueous phase on the extraction of Tl(III) by $[C_3C_1pyrr][Tf_2N]$ ionic liquid (closed symbols) and $[PDDA][Tf_2N]_n$ film (open and semi open symbols); the initial thallium concentration in the aqueous phase is $[Tl]_{aq,\ init}$ = $1.1 \cdot 10^{-5}$ M. The solid lines are for 1 M HCl and the dash dotted line is for 0.1 M HCl (shown for comparison). The lines are drawn according to Eq. 19.

It can be seen in Fig. 6 that in all cases, the slope is very close to –1. This indicates that for any HCl concentration in 0.1 – 1 M range, the predominant extracted species is $TlCl_4^-$. The intercepts allows for estimation of the ion exchange and ion pair formation constants. The results of this calculation for 1 M HCl (assuming only negatively charged thallium species in the aqueous phase) are given in Table 2.

Table 2 Calculated ion exchange and ion pair formation constants for Tl(III) extraction into ILs from 1 M HCl according to Eqs. 18 and 19

Constant	$[C_3C_1pyrr][Tf_2N]$	$[PDDA][Tf_2N]_n$
K_{IE}^*	$(3.8 \pm 0.4) \cdot 10^{-1}$	$(2.69 \pm 0.34) \cdot 10^{-3}$
K_{IP}	$(1.30 \pm 0.20) \cdot 10^{3}$	$> 2.3 \cdot 10^{4}$

* values were calculated for a fixed slope of –1

The values in Table 2 suggest that $TlCl_4^-$ is predominantly extracted in both cases via ion pair formation with the ILs' cation.

3.5.2 Tl(III) loading

The loading of stable metal should be considered to estimate the extraction capacity of the corresponding organic phase. Figure 6 shows distribution ratio values as a function of metal concentration in a 0.5 M HCl aqueous phase. Using the same principles considered in section 3.3, Eq. 8 must be modified to reflect the presence of stable Tl(III) in the system:

$$n \cdot [C_3C_1pyrr^{n+}]_{aq} - [Tf_2N^-]_{aq} = [HTf_2N]_{aq} + K_{ex\_HCl} \cdot [Cl^-]_{aq} + [C_3C_1pyrr^{n+}]_{aq} \cdot [Cl^-]_{aq}^n / K_{b\_ex\_C_3C_1pyrrCl_n} - \Delta[TlCl_4^-]_{aq}, \quad \text{Eq. 20}$$

where $\Delta[TlCl_4^-]_{aq}$ is the difference between the initial and equilibrium thallium concentrations in the aqueous phase. The solution to the corresponding quadratic equation is

$$[C_3C_1pyrr^+]_{aq} = \frac{K_{ex\_HCl}\cdot[Cl^-]_{aq} - \Delta[TlCl_4^-]_{aq} + \sqrt{\left(K_{ex\_HCl}\cdot[Cl^-]_{aq} - \Delta[TlCl_4^-]_{aq}\right)^2 + 4\cdot K_{sp}\cdot\left(1 - [Cl^-]_{aq}/K_{b\_ex\_C_3C_1pyrrCl}\right)}}{2\cdot\left(1 - [Cl^-]_{aq}/K_{b\_ex\_C_3C_1pyrrCl}\right)}$$

Eq. 21

Thus, the following equation

$$D_{Tl(III)} = \frac{K_{IP}\cdot[C_3C_1pyrr^+]_{aq}}{1 + K_5\cdot[Cl^-]_{aq}}$$

Eq. 22

can be used to fit the data in Fig. 7 for the $[C_3C_1pyrr][Tf_2N]$ ionic liquid, where $[C_3C_1pyrr^+]$ is described by Eq. 21. As can be seen, the Tl(III) distribution ratio for non-polymerized ionic liquid stays almost constant in the range of up to 10^{-2} M of stable thallium, and then decreases sharply with increasing metal concentration. However, the decrease in distribution ratio values for Tl(III) extracted by $[PDDA][Tf_2N]_n$ begins much earlier and there is an abrupt decline at approximately 10^{-3} M of stable thallium. This is most likely associated with the poly(IL) capacity, since the thallium concentration is greater than the concentration of dissolved $[PDDA][Tf_2N]_n$ ionic liquid ions.

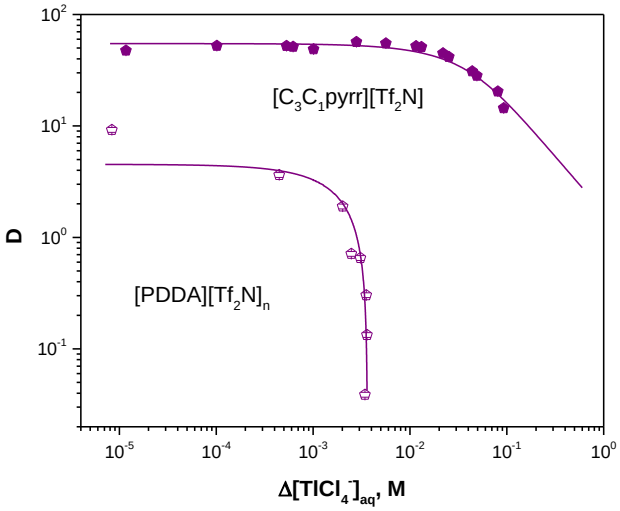

Fig. 7 Effect of $TlCl_3$ added to the 0.5 M HCl aqueous phase on the extraction of Tl(III) by $[C_3C_1pyrr][Tf_2N]$ ionic liquid (closed symbols) and $[PDDA][Tf_2N]_n$ film (open symbols). The lines are drawn according to Eqs. 22 and 24.

In order to fit the $[C_3C_1pyrr][Tf_2N]$ data based on eq. 22, it should be noted that extraction of the acid and back-extraction of $[C_3C_1pyrr]Cl$ ionic liquid is almost negligible at 0.5 M HCl, so we fixed the corresponding constants according to the data in Table 1: K_{ex_HCl} = 0.0179 and $K_{b\_ex\_C_3C_1pyrrCl} = 16.4$. As a result, the solubility product and ion pair formation constants were found to be K_{sp} = (1.19 ± 0.20) · 10^{-3} and K_{IP} = 1810 ± 180, and these values are in agreement with those estimated above.

It was obvious that the solubility of polymerized ionic liquid should be much less than that of regular IL due to the difficulties of the bulky poly-cation to be transferred to the aqueous phase. Now it is possible to compare the corresponding solubility products, and one can see that the solubility of $[PDDA][Tf_2N]_n$ is at least three orders of magnitude less than that of $[C_3C_1pyrr][Tf_2N]$. Comparison of the ion exchange and ion pair formation constants indicates that $TlCl_4^-$ is mostly extracted due to ion pair formation with

the pyrrolidinium-based cation. These results are in agreement with those we found for the [C_4mim][Tf_2N] imidazolium-based ionic liquid.[44]

In the case of polymerized ionic liquid, Langmuir and Freundlich adsorption isotherm equations[61] were considered and the former one was found to give the best fit (see Fig. S1 in Supplementary Information). The Langmuir equation is

$$S = \frac{K \cdot C}{b + C} \quad \text{Eq. 23}$$

where *S* is the amount adsorbed ($S = \Delta[TlCl_4^-]_{aq}$), *C* is the concentration of analyte in solution, and *b* and *K* are fitting constants. Thus, Eq. 23 in terms of distribution ratio is

$$D = \frac{K - \Delta[TlCl_4^-]_{aq}}{b} \quad \text{Eq. 24}$$

and the fitting parameters are $b = (8.1 \pm 1.0) \cdot 10^{-4}$ and $K = (3.64 \pm 0.07) \cdot 10^{-3}$.

3.6 Determination of thermodynamic parameters

The change in Gibb's energy (ΔG) can be calculated from the following equation:

$$\Delta G = -R \cdot T \cdot ln\, K \quad \text{Eq. 25}$$

where *R* is the gas constant and *T* is the temperature. The change in enthalpy (ΔH) and entropy (ΔS) during the extraction can be calculated according to the equation:

$$ln\, K = -\frac{\Delta H}{R \cdot T} + \frac{\Delta S}{R} \quad \text{Eq. 26}$$

A plot of *ln K* versus *1/T* gives a straight line with a slope of $-\Delta H/R$ and intercept of $\Delta S/R$.

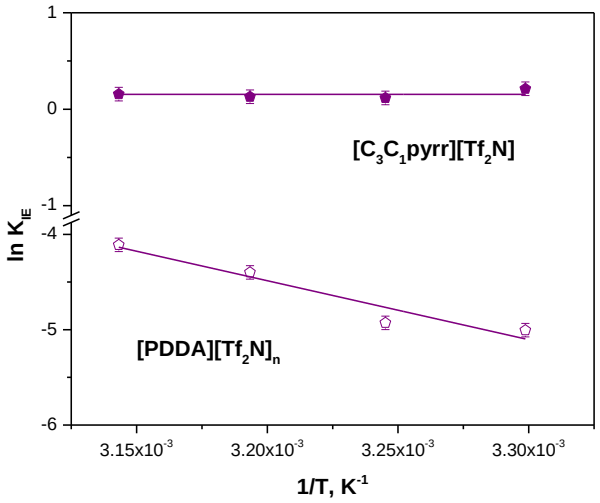

Fig. 8 Variation of Tl(III) equilibrium extraction constant values as a function of temperature. Extracting phase: [C_3C_1pyrr][Tf_2N] (closed symbols) and [PDDA][$Tf_2N]_n$ (open symbols). The solid-to-liquid phase ratio in the-case of solid phase extraction was

0.05 g/mL. The initial thallium concentration in the aqueous phase is $[Tl]_{aq,init}$ = 7.4·10^{-6} M, and extraction performed from 0.5 M HCl. The lines are drawn according to Eq. 26.

The extraction of 7.4·10^{-6} M Tl(III) from an aqueous acidic solution ([HCl] = 0.5 M) into $[C_3C_1pyrr][Tf_2N]$ ionic liquid in the 30 – 45 °C temperature range shows that the distribution ratio does not depend on the temperature. When similar experiments were carried out with a poly(ionic liquid) film, $[PDDA][Tf_2N]_n$, as an extraction phase, the distribution ratio values for Tl(III) were found to increase with increasing temperature (Fig. 8), indicating that the extraction process is endothermic. Table 3 contains calculated thermodynamic parameters for $[C_3C_1pyrr][Tf_2N]$ and $[PDDA][Tf_2N]_n$ ionic liquids.

Table 3 Calculated thermodynamic parameters for $[C_3C_1pyrr][Tf_2N]$ and $[PDDA][Tf_2N]_n$ in 0.5 M HCl

Parameter	$[C_3C_1pyrr][Tf_2N]$		$[PDDA][Tf_2N]_n$	
	Ion exchange	Ion pair	Ion exchange	Ion pair
ΔG_{298}, *kJ/mol*	2.38 ± 0.29	–17.78 ± 0.39	14.66 ± 0.32	< –24.90
ΔH, *kJ/mol*	0		51 ± 10	> 41
ΔS, *J/K/mol*	1.28 ± 0.18	66.17 ± 0.18	127 ± 32	> 227

Comparison of the values shown in Table 3 confirms that ion pair formation is the most favorable mechanism for Tl(III) extraction in the case of both regular and polymerized ionic liquids.

3.7 Extraction kinetics

The extraction kinetics of thallium from HCl solution onto a $[PDDA][Tf_2N]_n$ film was investigated in the range 0 – 60 min at a solid-to-liquid ratio of 0.05 g/mL and at fixed initial HCl concentration of 0.5 M. Examination of the time dependence of D_{Tl} (Fig. 9) shows that the distribution ratio reaches a plateau in approximately 30 minutes of shaking. Thus, the Tl(III) extraction kinetics in the solid-phase experiments with $[PDDA][Tf_2N]_n$ film is significantly slower than in the liquid-liquid extraction system with $[C_3C_1pyrr][Tf_2N]$ ionic liquid used as a pure extracting phase, in which the equilibrium is attained in less than 1 min.[44] This process is hindered due to the significantly lower solubility of bulky polymerized cation. In all experiments in the present study, the mixing time was maintained at 60 min to ensure extraction equilibrium.

First-order reaction kinetics is described as

$$C = C_0 \cdot e^{-k \cdot t} \qquad \text{Eq. 27}$$

and any higher order reaction as

$$C^{1-n} = C_0^{1-n} + (n-1) \cdot k \cdot t \qquad \text{Eq. 28}$$

where C and C_0 are current and initial aqueous concentration of the analyte, k is the rate constant, t is time of the process, and n is order of the reaction. Taking both Eqs. 27 and 28 into account, the best fit (R^2 = 0.99979) of our experimental data for the polymerized ionic liquid revealed that a 4th order reaction occurs, n = 4.30 ± 0.31 and k = (2.25 ± 0.19) · 10^{16} M^{-3}·min^{-1} (see Fig. S2 in Supplementary Information). Thus, the corresponding equation in terms of distribution ratio is

$$D = C_0 \cdot (3 \cdot k \cdot t + C_0^{-3})^{1/3} - 1 \qquad \text{Eq. 29}$$

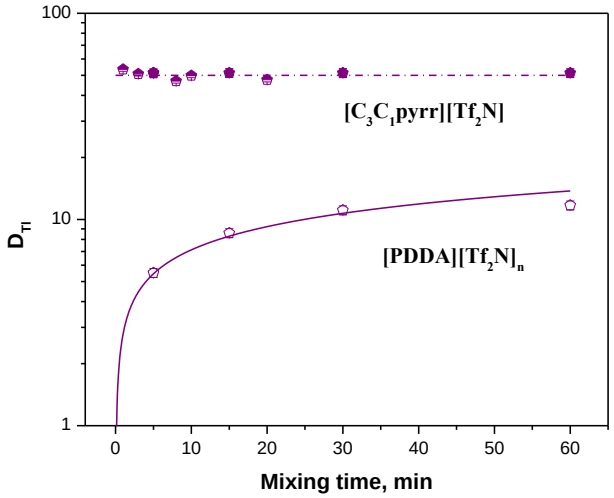

Fig. 9 Effect of mixing time on the extraction of Tl(III) from 1 M and 0.5 M HCl feed solution with ionic and poly(ionic liquid), $[C_3C_1pyrr][Tf_2N]$ and $[PDDA][Tf_2N]_n$, respectively. In the case of solid-liquid extraction, the solid-to-liquid phase ratio is 0.05 g/mL. The initial concentration of Tl(III) in the aqueous phase is $9.3 \cdot 10^{-6}$ M. Data for a non-polymerized IL (semi open symbols), where carrier-free thallium was oxidized by chlorine water, are taken from our previous article.[44] The solid line is drawn according to the Eq. 29.

3.8 Acidity dependent Tl(III) extraction

Extraction of Tl(III) by means of the polymer was studied as a function of HCl concentration, and the results observed are shown in Fig. 10.

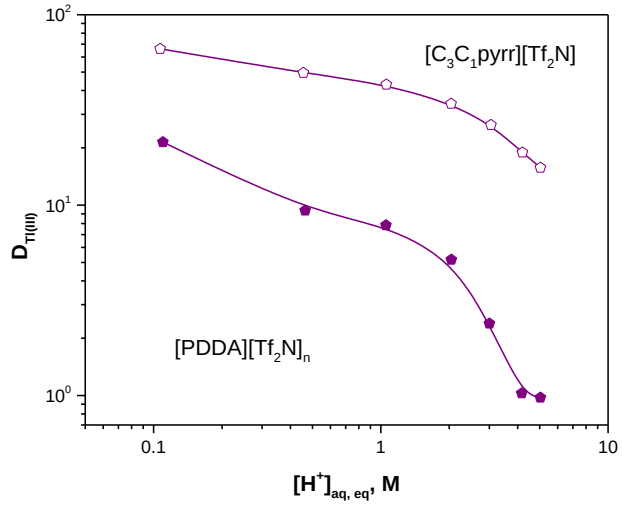

Fig. 10 Effect of HCl concentration on Tl(III) extraction into IL and poly(IL) phases. In the case of solid-liquid extraction, the solid-to-liquid phase ratio is 0.05 g/mL. The initial concentration of Tl(III) in the aqueous phase is $9.3 \cdot 10^{-6}$ M. The lines are drawn to guide the eye.

Figure 9 clearly indicates that the distribution ratio values of Tl(III) extracted by the polymer are generally below those of the non-polymerized IL. However, the corresponding D values are greater than 1 over the entire HCl range considered, and greater than 10 in the low-acidity region for both organic

phases; this results in efficient extraction, especially from < 1 M HCl. The mechanism of Tl(III) extraction described above indicates that the $TlCl_4^-$ species is extracted in the form of ion pairs with the corresponding IL cation. Thus, the decrease of D values with increasing acid concentration is related to formation of a non-extracted higher complex, namely $TlCl_5^{2-}$.

4 Conclusion

Polymerized pyrrolidinium-based ionic liquid has been utilized to coat the inner surface of a plastic (PTFE) tube alone and a tube filled with glass beads. The rotary evaporation of the solvent, which the poly(IL) is dissolved in, allows for formation of a uniform and non-porous layer on the tube wall. Such a solid film successfully maintains glass beads, forming a pseudomonolithic column with open pores. This film retains the chemical properties of its non-polymerized pyrrolidinium-based analog. The polymer can adsorb the same metal in the same oxidation state as the regular ionic liquid. However, the poly(IL) shows almost 100 times slower kinetics than the IL. Also, due to the bulky polymerized cation, its solubility in the aqueous phase is very limited and this affects the metal extraction. Despite that, Tl(III) distribution ratios in case of poly(IL) are several times lower than those of the regular ionic liquid, and these *D* values in both cases are greater than 10 in the low-acidity region. This means that both polymerized and non-polymerized ionic liquids can reach 90% extraction efficiency. A mathematical method has been used to estimate the solubility of both ionic liquids in the aqueous phase and to shed light on the mechanism of Tl(III) extraction. The data reveal that the solubility product constant of the poly(IL) is at least three orders of magnitude lower than that of the IL. Also, it was shown that both ionic liquids extract thallium in the form of $TlCl_4^-$, and ion pair formation between this species and the ionic liquid cation is the primary mechanism of extraction. This conclusion is based on a comparison of the calculated thermodynamic constants and changes in Gibbs energy for each process. These results show that the process favors ion pair formation.

Conflicts of interest

There are no conflicts to declare.

Acknowledgements

Financial support from the National Center for Scientific Research (CNRS, France) through its International Program for Scientific Cooperation (PICS) is gratefully acknowledged. The authors thank M. Coppe, Dr. L. Allouche and Dr. B. Vincent (Institute of Chemistry, University of Strasbourg, France) for the NMR measurements, and S. Georg and Dr. O. Courson (IPHC, France) for ICP-MS measurements. The authors thank Dr. Y. Bisrat for the SEM measurements at the Texas A&M University Materials Characterization Facility. This material is based upon work supported by the U.S. Department of Energy, Office of Science, Office of Nuclear Physics under Award No. DE-FG02-93ER40773. This material is based upon work supported by the Department of Energy National Nuclear Security Administration through the Nuclear Science and Security Consortium under Award Number DE-NA0003180. This report was prepared as an account of work sponsored by an agency of the United States Government. Neither the United States Government nor any agency thereof, nor any of their employees, makes any warranty,

express or implied, or assumes any legal liability or responsibility for the accuracy, completeness, or usefulness of any information, apparatus, product, or process disclosed, or represents that its use would not infringe privately owned rights. Reference herein to any specific commercial product, process, or service by trade name, trademark, manufacturer, or otherwise does not necessarily constitute or imply its endorsement, recommendation, or favoring by the United States Government or any agency thereof. The views and opinions of authors expressed herein do not necessarily state or reflect those of the United States Government or any agency thereof.

Notes and references

1. P. Patnaik, *A Comprehensive Guide to the Hazardous Properties of Chemical Substances*, John Wiley & Sons, Inc., Hoboken, New Jersey, Third edn., 2007.
2. F. Endres and S. Zein El Abedin, *Phys. Chem. Chem. Phys.*, 2006, **8**, 2101-2116.
3. S. T. Handy, *Applications of ionic liquids in science and technology*, InTech, Rijeka, Croatia, 2011.
4. A. P. de los Rios, F. J. Hernandez-Fernandez, F. J. Alguacil, L. J. Lozano, A. Ginesta, I. Garcia-Diaz, S. Sanchez-Segado, F. A. Lopez and C. Godinez, *Sep. Purif. Technol.*, 2012, **97**, 150-157.
5. N. Papaiconomou, G. Vite, N. Goujon, J.-M. Lévêque and I. Billard, *Green Chem.*, 2012, **14**, 2050-2056.
6. L. A. Schaider, S. A. Balan, A. Blum, D. Q. Andrews, M. J. Strynar, M. E. Dickinson, D. M. Lunderberg, J. R. Lang and G. F. Peaslee, *Environ. Sci. Technol. Lett.*, 2017, **4**, 105-111.
7. A. Blum, S. A. Balan, M. Scheringer, X. Trier, G. Goldenman, I. T. Cousins, M. Diamond, T. Fletcher, C. Higgins, A. E. Lindeman, G. Peaslee, P. de Voogt, Z. Wang and R. Weber, *Environ. Health Perspect.*, 2015, **123**, A107-111.
8. M. Fan, L. Ma, C. Zhang, Z. Wang, J. Ruan, M. Han, Y. Ren, C. Zhang, D. Yang, F. Zhou and W. Liu, *Tribology Transactions*, 2017, 1-12.
9. D. Parmentier, T. Vander Hoogerstraete, S. J. Metz, K. Binnemans and M. C. Kroon, *Ind. Eng. Chem. Res.*, 2015, **54**, 5149-5158.
10. N. N. Hidayah and S. Z. Abidin, *Miner. Eng.*, 2017, **112**, 103-113.
11. M. M. Hassanien, W. I. Mortada, I. M. Kenawy and H. El-Daly, *Appl. Spectrosc.*, 2017, **71**, 288-299.
12. E. Andrzejewska, *Polym. Int.*, 2017, **66**, 366-381.
13. A. Eftekhari and T. Saito, *Eur. Polym. J.*, 2017, **90**, 245-272.
14. D. J. S. Patinha, L. C. Tome, M. Isik, D. Mecerreyes, A. J. D. Silvestre and I. M. Marrucho, *Materials*, 2017, **10**, 1094.
15. H. Piri-Moghadam, M. N. Alam and J. Pawliszyn, *Anal. Chim. Acta*, 2017, **984**, 42-65.
16. L. Vidal, M. L. Riekkola and A. Canals, *Anal. Chim. Acta*, 2012, **715**, 19-41.
17. C. F. Poole and N. Lenca, *J. Chromatogr. A*, 2014, **1357**, 87-109.
18. X. Liu, F. Suo, M. He, B. Chen and B. Hu, *Microchim. Acta*, 2017, **184**, 927-934.
19. Z. Ji, R. E. Majors and E. J. Guthrie, *J. Chromatogr. A*, 1999, **842**, 115-142.
20. C. Shen, Y. Wang, J. Xu and G. Luo, *Chem. Eng. J.*, 2013, **229**, 217-224.
21. X.D. Liu, S. Tokura, M. Haruki, N. Nishi and N. Sakairi, *Carbohydr. Polym.*, 2002, **49**, 103-108.
22. J.A. Buono, R.W. Karin and O. Fasching, *Anal. Chim. Acta*, 1975, **80**, 327-334.
23. Bouche J. and Verzele M., *J. Chromatogr. Sci.*, 1968, **6**, 501-505.
24. Alexander G., Garzó G. and Pályi G., *J. Chromatogr. A*, 1974, **91**, 25-37.
25. M. Novotný and A. Zlatkis, *Chromatogr. Rev.*, 1971, **14**, 1-44.
26. G. A. F. M. Rutten and J. A. Luyten, *J. Chromatogr. A*, 1972, **74**, 177-193.

27. M. Souada, C. Louage, J. Y. Doisy, L. Meunier, A. Benderrag, B. Ouddane, S. Bellayer, N. Nuns, M. Traisnel and U. Maschke, *Ultrason. Sonochem.*, 2018, **40**, 929-936.
28. W. I. Mortada, I. M. Kenawy and M. M. Hassanien, *Anal. Methods*, 2015, **7**, 2114-2120.
29. N. Belzile and Y.-W. Chen, *Appl. Geochem.*, 2017, **84**, 218-243.
30. A. Miyazaki, A. Kimura and H. Tao, *Bull. Environ. Contam. Toxicol.*, 2012, **89**, 1211-1215.
31. V. Drozdovitch, A. B. Brill, R. J. Callahan, J. A. Clanton, A. DePietro, S. J. Goldsmith, B. S. Greenspan, M. D. Gross, M. T. Hays, S. C. Moore, J. A. Ponto, W. W. Shreeve, D. R. Melo, M. S. Linet and S. L. Simon, *Health Phys.*, 2015, **108**, 520-537.
32. G. Barone-Rochette, F. Zoreka, L. Djaileb, N. Piliero, A. Calizzano, J. L. Quesada, A. Broisat, L. Riou, J. Machecourt, D. Fagret, G. Vanzetto and C. Ghezzi, *J. Nucl. Cardiol.*, 2018, DOI: 10.1007/s12350-018-1189-8, 1-11.
33. G. Repetto and A. del Peso, in *Patty's Toxicology*, John Wiley & Sons, Inc., 2001, ch. 10.
34. J. J. Rodriguez-Mercado and M. A. Altamirano-Lozano, *Drug Chem. Toxicol.*, 2013, **36**, 369-383.
35. J. H. Lee, D. J. Kim and B. K. Ahn, *Bull. Environ. Contam. Toxicol.*, 2015, **94**, 756-763.
36. D. Mecerreyes, *Prog. Polym. Sci.*, 2011, **36**, 1629-1648.
37. W. Qian, J. Texter and F. Yan, *Chem. Soc. Rev.*, 2017, **46**, 1124-1159.
38. Z. Xu, Y. Zhao, P. Wang, X. Yan, M. Cai and Y. Yang, *Ind. Eng. Chem. Res.*, 2019, **58**, 1779-1786.
39. X. Briones O, R. A. Tapia, P. R. Campodónico, M. Urzúa, Á. Leiva, R. Contreras and J. González-Navarrete, *React. Funct. Polym.*, 2018, **124**, 64-71.
40. E. E. Tereshatov, M. Y. Boltoeva and C. M. Folden III, *Solvent Extr. Ion Exch.*, 2015, **33**, 607-624.
41. F. W. E. Strelow, A. H. Victor, C. R. van Zyl and C. Eloff, *Anal. Chem.*, 1971, **43**, 870-876.
42. I. Billard and S. Georg, *Helv. Chim. Acta*, 2009, **92**, 2227-2237.
43. V. Mazan, M. Y. Boltoeva, E. E. Tereshatov and C. M. Folden III, *RSC Adv.*, 2016, **6**, 56260-56270.
44. E. E. Tereshatov, M. Y. Boltoeva, V. Mazan, M. F. Volia and C. M. Folden III, *J. Phys. Chem. B*, 2016, **120**, 2311-2322.
45. S. Katsuta, Y. Watanabe, Y. Araki and Y. Kudo, *ACS Sustainable Chem. Eng.*, 2016, **4**, 564-571.
46. M. F. Volia, E. E. Tereshatov, V. Mazan, C. M. Folden III and M. Boltoeva, *J. Mol. Liq.*, 2019, **276**, 296-306.
47. B. P. Nikolsky, in *Chemical Equilibrium and Kinetic, Property of Solutions, Electrode Processes*, Chemistry, Leningrad, 1965 (in Russian), vol. 3, ch. Activity Coefficients, p. 1008.
48. V. Mazan, I. Billard and N. Papaiconomou, *RSC Adv.*, 2014, **4**, 13371-13384.
49. C. Gaillard, V. Mazan, S. Georg, O. Klimchuk, M. Sypula, I. Billard, R. Schurhammer and G. Wipff, *Phys. Chem. Chem. Phys.*, 2012, **14**, 5187-5199.
50. X. Q. Sun, H. M. Luo and S. Dai, *Chem. Rev.*, 2012, **112**, 2100-2128.
51. M. P. Jensen, J. Neuefeind, J. V. Beitz, S. Skanthakumar and L. Soderholm, *J. Am. Chem. Soc.*, 2003, **125**, 15466-15473.
52. C. H. C. Janssen, A. Sanchez, G. J. Witkamp and M. N. Kobrak, *Chemphyschem*, 2013, **14**, 3806-3813.
53. S. A. Ansari, P. K. Mohapatra, V. Mazan and I. Billard, *RSC Adv.*, 2015, **5**, 35821-35829.
54. T. Sun, X. Shen and Q. Chen, *Sci. China Chem.*, 2013, **56**, 782-788.
55. T. Sato, *Shigen-to-Sozai*, 1996, **112**, 123-128.
56. K. Schmidt, *J. Inorg. Nucl. Chem.*, 1970, **32**, 3549-3557 (in German).
57. I. Banyai and J. Glaser, *J. Am. Chem. Soc.*, 1989, **111**, 3186-3194.
58. S. Katsuta, K. Nakamura, Y. Kudo and Y. Takeda, *J. Phys. Chem. B*, 2012, **116**, 852-859.
59. Y. Watanabe and S. Katsuta, *J. Chem. Eng. Data*, 2014, **59**, 696-701.
60. T. Hamamoto, M. Okai and S. Katsuta, *J. Phys. Chem. B*, 2015, **119**, 6317-6325.
61. J. Skopp, *J. Chem. Educ.*, 2009, **86**, 1341-1343.

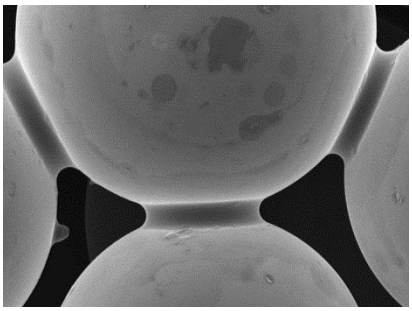

To our knowledge, there are a few articles on polymerized ionic liquids application for metal extraction from aqueous solutions.